

# Magnetic, magnetocaloric and optical properties of nano $\text{Gd}_3\text{Ga}_5\text{O}_{12}$ garnet synthesized by citrate sol-gel method

Chalappurath Pattelath Reshmi<sup>1,\*</sup> , Analiparambil Ravindran Ramesh<sup>1,\*</sup> ,  
Athira Suresh<sup>2</sup> , Deepshikha Jaiswal-Nagar<sup>2</sup> 

<sup>1</sup>Department of Chemistry, Government Victoria College, Research Center under University of Calicut, Palakkad, India.

<sup>2</sup>School of Physics, IISER Thiruvananthapuram, Vithura, Thiruvananthapuram, India.

\*Corresponding authors: [cpreshmi@gvc.ac.in](mailto:cpreshmi@gvc.ac.in), [aroramesh@gvc.ac.in](mailto:aroramesh@gvc.ac.in)

## Original Research

Received:  
29 August 2024  
Revised:  
25 October 2024  
Accepted:  
29 October 2024  
Published online:  
1 April 2025

© 2025 The Author(s). Published by the OICC Press under the terms of the [Creative Commons Attribution License](https://creativecommons.org/licenses/by/4.0/), which permits use, distribution and reproduction in any medium, provided the original work is properly cited.

## Abstract:

$\text{Gd}_3\text{Ga}_5\text{O}_{12}$  (GGG) nanoparticles with an average size around 50 nm were synthesized via citrate sol-gel method. Rietveld refinement confirmed the formation of a single-phase garnet structure. The optical properties characterized by UV-Vis absorption and photoluminescence spectra, exhibited bands centered at 300 nm and 436 nm, respectively. Magnetic measurements revealed paramagnetic behaviour above 15 K, as evidenced by the modified Curie-Weiss fitting with an effective magnetic moment of 13.86  $\mu\text{B}$  per formula unit (F. U.). Arrott plots confirmed a second-order nature of the magnetic phase transition. Notably, the GGG nanoparticles displayed a significant magnetocaloric effect (MCE), with a maximum magnetic entropy change ( $-\Delta\text{SM}$ ) of 14.2  $\text{Jkg}^{-1}\text{K}^{-1}$  at 3.5 K under a 5 T field. These findings highlight the potential of GGG nanoparticles as refrigerants for low temperature magnetic refrigeration applications.

**Keywords:** Arrott plot; Effective magnetic moment; Magnetocaloric effect (MCE); Nano GGG; Optical properties; Rietveld refinement

## 1. Introduction

Rare earth (RE) based garnets, with their general formula  $\text{A}_3\text{B}_2\text{C}_3\text{O}_{12}$  ( $\text{A} = \text{RE}^{3+}$ , B and C =  $\text{Fe}^{3+}/\text{Al}^{3+}/\text{Ga}^{3+}$ ), have emerged as a class of materials with exceptional magnetic, electrical, and optical properties [1, 2]. Their cubic crystal structure ( $Ia\bar{3}d$ ), characterized by dodecahedral, octahedral, and tetrahedral sites, enables the accommodation of diverse cations [3–5]. This structural flexibility has led to their extensive application in optical components like modulators and magnetic field sensors [6]. Beyond their optical properties, the magneto-optical characteristics of ferrimagnetic garnets have garnered significant attention. The interplay between light and magnetization offers a powerful tool for visualizing magnetic domain structures and magnetization distributions, crucial for advancing technologies such as magnetic bubble memory [7, 8].

Rare earth garnets experienced a resurgence with the discovery of the magnetocaloric effect (MCE) in  $\text{RE}_3(\text{Ga/Fe})_5\text{O}_{12}$  by Belov *et al.*, which describes a material's ability to heat or cool in response to magnetic field changes [9, 10]. MCE,

quantified by isothermal entropy change ( $\Delta S_M$ ) or adiabatic temperature change ( $\Delta T_{ad}$ ), holds immense potential for magnetic refrigeration applications operating near liquid helium temperatures, where traditional gas compression based refrigeration methods become inefficient [11]. The current challenge is to identify safer alternatives that minimize environmental impact while maintaining energy efficiency in active heating and cooling systems [12]. Consequently, a diverse array of magnetic solids, such as complex oxides [13–15], rare earth-transition metal alloys [16] and rare earth transition metal carbides [17] have been developed in recent years. Gadolinium Gallium Garnet (GGG) has become a benchmark refrigerant for temperatures below 20 K due to its favourable properties [11, 18]. The large magnetic moment of  $\text{Gd}^{3+}$  ions and the crystallographic structure of GGG contribute to its promising magnetocaloric properties [19]. Recently, Xiang Jin *et al.* investigated the effects of high pressure heat treatment on GGG single crystals, revealing enhanced magnetic refrigeration power and a broadened phase transition temperature range [20]. Researchers have extensively studied gadolinium gallium

garnets, substituting Gd with Dy or Ho and Ga with Fe to enhance magnetocaloric properties. The substitution of Gd with Dy or Ho in GGG creates superparamagnetic materials with fine clusters. This substitution notably enhances the magnetocaloric effect [21]. Phan *et al.* studied the MCE of bulk and nano  $\text{Gd}_3\text{Fe}_5\text{O}_{12}$  garnet. The nanostructured gadolinium iron garnets exhibit a complex MCE behaviour compared to their bulk counterparts, influenced by factors such as grain size, surface spin disorder, and magnetic frustration [22].

GGG possesses a complex crystal structure with  $\text{Gd}^{3+}$  ions located on two interpenetrating corner-sharing triangular sublattices. This arrangement leads to geometric frustration in GGG, which prevents the establishment of long-range antiferromagnetic order. The frustration results in unique magnetic behaviours, making GGG a fascinating material for the study of frustrated magnetism [23–25]. GGG also exhibits noteworthy magneto-optical properties due to the presence of gadolinium ions with a substantial magnetic moment. This makes GGG a valuable material for faraday rotators and isolators in laser technology, where the rotation of the polarization plane of light in a magnetic field is utilized. GGG's transparency across the visible and near-infrared spectrum further enhances its suitability for optical devices [26–28].

However, the synthesis of high quality GGG is crucial for optimizing its optical and magnetocaloric properties. Traditional solid state methods often result in inhomogeneous materials with limited control over particle size and morphology. Synthesis of GGG is challenging due to the need of high temperatures, around 1300 °C, and extended durations ranging from 12 to 48 hours [29]. A wide variety of wet chemical methods have been developed for low temperature synthesis of nanomaterials with tunable magnetic and optical properties [30, 31]. This study aims to optimize the synthesis of high quality GGG nanoparticles by citrate sol-gel method [32] and comprehensively characterize their structural, optical, magnetic, and magneto-thermal properties. By understanding the interplay between GGG's optical and magnetocaloric characteristics, we seek to contribute to the development of advanced materials for both magnetic refrigeration and optical applications.

## 2. Methods

### 2.1 Synthesis of nano GGG by citrate sol-gel method

High purity gadolinium (III) oxide ( $\text{Gd}_2\text{O}_3$ , Sigma-Aldrich, 99.9%) and gallium (III) oxide ( $\text{Ga}_2\text{O}_3$ , Sigma-Aldrich, 99.99%) were accurately weighed in the specified mole ratio and separately dissolved in concentrated nitric acid ( $\text{HNO}_3$ ). Upon dissolution, the oxides were converted into their corresponding nitrates. To the resulting homogeneous solution of  $\text{Gd}^{3+}$  and  $\text{Ga}^{3+}$  nitrates, citric acid and ethylene glycol were added as complexing agents. The entire mixture was then heated at 90 °C for four hours with continuous stirring using a magnetic stirrer to form a gel. The gel was charred, resulting in the formation of a fine precursor powder, which was then ground and calcined at 750 °C for 2 hours to obtain pure nano GGG.

### 2.2 Characterisation of nano GGG

The X-ray diffraction (XRD) pattern of nano GGG was recorded using a PANalytical X'Pert Pro diffractometer configured in Bragg-Brentano geometry with copper  $K\alpha$  radiation. The scan was conducted in the  $2\theta$  range of  $10^\circ$  to  $90^\circ$  with a step size and scan step time of  $0.017^\circ$  and 40.702 seconds, respectively. Particle morphology was studied using High Resolution Transmission Electron Microscopy (FEI Tecnai G2 30 EDAX). The magnetization was measured as a function of temperature and applied magnetic field using a Quantum Design's SQUID (Superconducting Quantum Interference Device) magnetometer (Model MPMS3). The magnetization data were employed to derive isothermal magnetic entropy change ( $-\Delta S_M$ ) through the application of integrated Maxwell's relation [18].

$$\Delta S_M = \frac{\int_0^H M(T + \Delta T, H') dH' - \int_0^H M(T, H') dH'}{\Delta T} \quad (1)$$

The ultraviolet-visible absorption spectrum was measured using a Shimadzu UV-3600 double beam spectrophotometer. Emission spectrum of the nano GGG powder was recorded using a Jobin Yvon SPEX-Fluorolog 3 (Horiba) spectrofluorometer. A 450 W xenon arc lamp served as the excitation light source. Both excitation and emission monochromators were employed and emitted photons were detected using a photomultiplier tube detector.

## 3. Results and discussion

The recorded X-ray diffraction pattern of nano GGG was initially analyzed with the JCPDS file no-71-0701 to verify phase formation, with the indexed pattern presented in Fig. 1 (a) [26]. Subsequently, the XRD pattern was refined using Rietveld refinement with GSAS software [33]. The background was fitted using a shifted Chebyshev polynomial with 10 variables. The refined structural parameters confirm the presence of a single-phase garnet structure with the ( $Ia\bar{3}d$ ) space group. Figure 1 (b) presents the observed, calculated, and difference XRD patterns of nano GGG after refinement, while the various structural parameters are listed in Table 1. As reported in the literature, the XRD pattern of nano GGG shows peak broadening, which is attributed to the larger surface-to-volume ratio of the nanoparticles [34]. To determine the crystallite size using XRD, a Gaussian fit was applied to the (420) peak, as shown in Fig. 1 (c). The crystallite size of nano GGG was calculated to be 16.10 nm using the Debye-Scherrer formula,  $D = K\lambda/\beta \cos \theta$  [35, 36]. Figures 2 (a) and 2 (b) depict the TEM image and SAED pattern of nano GGG, respectively, revealing the agglomerated nature of the particles with an approximate size of 50 nm. Magnetic nanoparticles can experience dipole-dipole interactions, where the magnetic moments of different particles attract each other. This magnetic attraction can cause the nanoparticles to come together and agglomerate [37, 38]. Figure 3 (a) presents the absorption spectrum of synthesized nano GGG, exhibiting a maximum at 300 nm and the absorption band spans from 250 nm to 350 nm, resulting in a transparent window encompassing the visible and near-infrared regions of the electromagnetic spectrum. As depicted in Fig. 3 (b), the photoluminescence of nano GGG

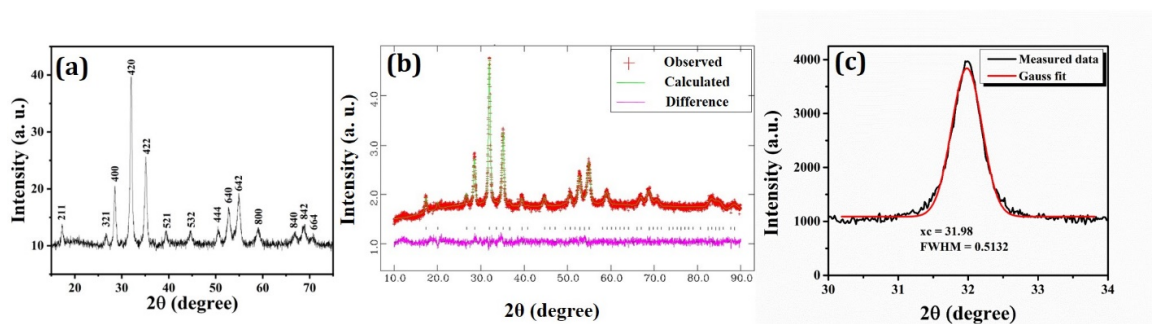


**Figure 1.** (a). Indexed XRD pattern of nano GGG synthesised by citrate sol-gel method (JCPDS file no-71-0701), (b) Rietveld refined XRD pattern of nano GGG and, (c) Detailed view of the (420) XRD peak with corresponding Gaussian fit overlay

**Table 1.** Structural parameters of nano sized Gd<sub>3</sub>Ga<sub>5</sub>O<sub>12</sub>.

| Material                  | Nano GGG    |
|---------------------------|-------------|
| Space group               | <i>Ia3d</i> |
| Lattice parameter, a (°A) | 12.4852 (3) |
| Volume (°O <sup>3</sup> ) | 1946.2 (1)  |
| Atomic positions          |             |
| Gd x                      | 0.125       |
| Gd y                      | 0           |
| Gd z                      | 0.25        |
| Ga1 x                     | 0           |
| Ga1 y                     | 0           |
| Ga1 z                     | 0           |
| Ga2 x                     | 0.375       |
| Ga2 y                     | 0           |
| Ga2 z                     | 0.25        |
| O x                       | -0.0348 (3) |
| O y                       | 0.0579 (1)  |
| O z                       | 0.1641 (4)  |
| Goodness of fit           |             |
| Rwp %                     | 2.27        |
| Rp %                      | 1.80        |

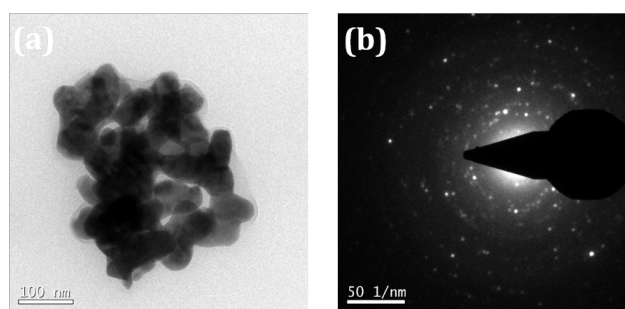


**Figure 2.** (a). TEM image and, (b) SAED pattern of nano GGG.

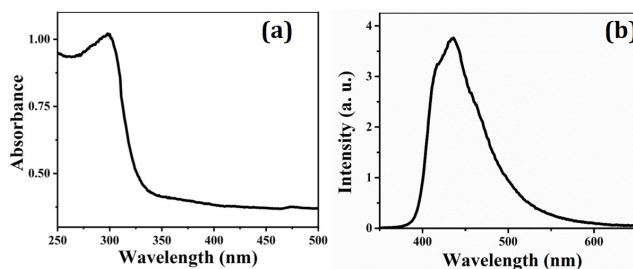


**Figure 3.** (a). Absorption spectrum and (b) Emission spectrum ( $\lambda_{exc}$  340 nm) of nano GGG.

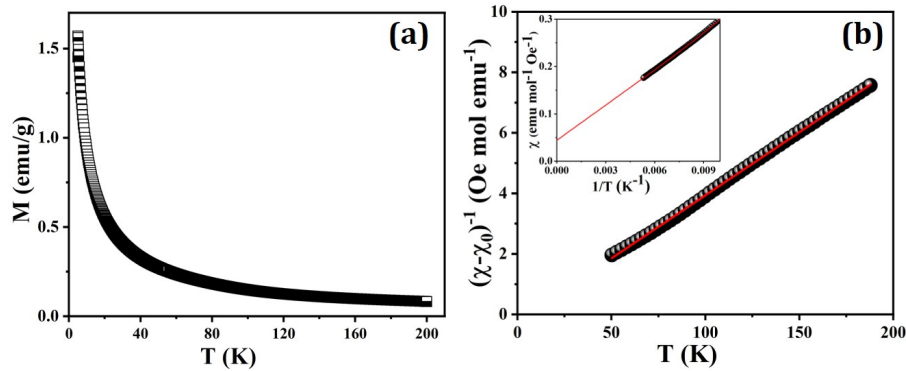


**Figure 4.** (a). M-T curve of nano GGG at 0.05 T, (b) Modified Curie-Weiss law fit of nano GGG and, ((4 b) inset) Determination of  $\chi_0$  from the plot of  $\chi$  vs.  $1/T$ .

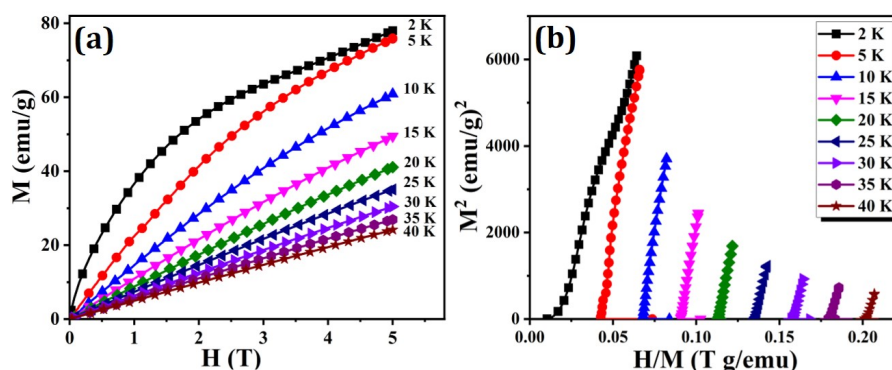
displays a broad emission band centered at 436 nm, extending from 375 to 600 nm. Previous studies have reported similar broad band blue photoluminescence, which is attributed to  $\text{Ga}_2\text{O}_3$  [39].

Figure 4 (a) represents the temperature dependence of magnetization of nano GGG in a magnetic field of 0.05 T. The data reveal a sharp increase in magnetization below 20 K, indicating magnetic ordering within the rare earth magnetic sublattice [40–42]. In the garnet structure,  $\text{Gd}^{3+}$  ions form a frustrated 3D network of corner-sharing triangles. This prevents antiferromagnetic interactions from being fully satisfied, leaving the system in a disordered state. This results in high magnetization at low temperatures [43–46]. In order to determine the effective magnetic moment, modified Curie-Weiss (C-W) fit was performed over the temperature range of 50 K to 200 K using the equation,  $\chi = \chi_0 + C/(T - \theta_{cw})$  [42]. The temperature-independent susceptibility is denoted by  $\chi_0$ , C represents the Curie-Weiss constant, while  $\theta_{cw}$  is the Curie-Weiss temperature associated with the paramagnetic moment. The Fig. 4 (b) shows the plot of  $(\chi - \chi_0)^{-1}$  vs.  $T$ , which suggests paramagnetic behaviour of nano GGG. The temperature independent susceptibility ( $\chi_0$ ) was determined from the plot of susceptibility ( $\chi$ ) vs.  $1/T$  as shown in the inset of Fig. 4 (b). The effective magnetic moment, calculated using the formula  $\mu_{eff} = \sqrt{8C}$ , is found to be  $13.86 \mu\text{B} / \text{F. U.}$ , which is in direct agreement with the theoretical value of  $13.75 \mu\text{B} / \text{F. U.}$  of bulk GGG reported in the literature [47, 48].

Magnetization curves of nano GGG were recorded at dif-

ferent temperatures near the transition point (Fig. 5 (a)) to explore the variation in the magnetocaloric effect. At 2 K, the M-H curve of nano GGG exhibits significant magnetization even at low fields and remains unsaturated up to a field of 5 T, indicating the frustrated magnetic state of the sample, whereas, the linear field dependence of magnetization above 15 K, signifies the paramagnetic behaviour of nano GGG. To determine the nature of magnetic phase transition, the Arrott plots ( $M^2$  vs.  $H/M$ ) for nano GGG are presented in Fig. 5 (b). Arrott plots with a positive slope indicate a second-order phase transition, while those with a negative slope imply a first-order transition [49]. The Arrott plots for nano GGG reveal linear isotherms with positive slopes, confirming the second-order nature of the phase transition. From the M-H data, the magnetic entropy change was calculated using Equation 1 at various magnetic field strengths, as depicted in Fig. 6 (a). The results show that the magnetic entropy change ( $-\Delta S_M$ ) increases with the field strength, with the maximum observed value of  $-\Delta S_M$  for nano GGG being  $14.2 \text{ J/kgK}$  at 3.5 K under a 5 T magnetic field. This suggests that nano GGG has potential as a refrigerant for low temperature magnetic refrigeration applications.

The field dependent magnetic entropy change is a key characteristic that provides valuable critical information into the magnetic behaviour of materials, particularly concerning magnetic refrigeration applications and magnetocaloric effects. This dependence typically follows a power-law relationship, with the exponent ( $n$ ), varying depending on whether the material is in the low temperature frustrated



**Figure 5.** (a). Field dependant magnetization and, (b) Arrott plots of nano GGG.

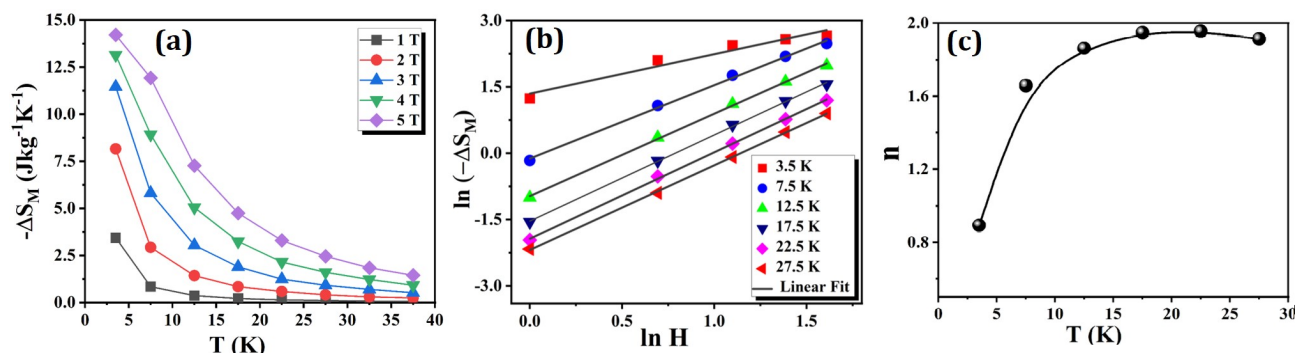


**Figure 6.** (a). Temperature dependence of magnetic entropy change, (b) Linear plots of  $\ln(-\Delta S_M)$  vs.  $\ln(H)$  at various temperatures and (c) Temperature dependence of exponent,  $n$  of nano GGG.

state, near the critical temperature, or in the high temperature paramagnetic region. Direct integration of the Curie-Weiss law for ferromagnetic materials above their Curie temperature yields an exponent of  $n = 2$ . In contrast, a mean-field approach predicts that the magnetic entropy change at the Curie temperature will have a field dependence characterized by  $n = 2/3$  [50]. A linear relationship between  $\ln(-\Delta S_M)$  and  $\ln(H)$  was investigated for temperatures ranging from 3.5 K to 27.5 K (Fig. 6 (b)). The slope of these plots determined the value of  $n$ , which was subsequently plotted against temperature for nano GGG (Fig. 6 (c)). The results indicate that the exponent “ $n$ ” ranges from 0.89 to 1.96, suggesting significant magnetic ordering in nano GGG at low temperatures.

#### 4. Conclusion

This study demonstrates the successful synthesis of  $Gd_3Ga_5O_{12}$  (GGG) nanoparticles using a low temperature, short duration process, optimized for magnetocaloric applications. The particles exhibited a uniform size around 50 nm and a pure garnet phase, as confirmed by TEM and Rietveld refinement, respectively. Optical studies revealed characteristic absorption and emission bands. Magnetic measurements indicated paramagnetic behaviour at higher temperatures. The magnetic phase transition was confirmed to be second-order by Arrott plots. Most importantly, the GGG nanoparticles displayed a considerable magnetocaloric effect, with a maximum  $-\Delta S_M$  of 14.2 J/kgK at 3.5 K under a 5 T field. These results highlight the potential of GGG nanoparticles as a promising material for magnetic refrigeration at low temperatures. Further investigations aimed at enhancing the magnetocaloric properties through size and compositional engineering are warranted.

#### Acknowledgments

C.P.R. thank UGC for the funding (minor research project No. 2223-MRP/15-16/KLCA009/ UGC-SWRO).

#### Authors contributions

Authors have contributed equally in preparing and writing the manuscript.

#### Availability of data and materials

The authors declare that the data supporting the findings of this study are available from the corresponding author upon reasonable request.

#### Conflict of interests

The authors declare no conflict of interest.

#### References

- [1] V. I. Nizhankovskiy. “Comparison of magnetic moment and magnetostriction of  $Gd_3Ga_5O_{12}$  and  $Tb_3Ga_5O_{12}$  single crystals.”. *J. Alloys. Compd.*, 852:156938–156943, 2021. DOI: <https://doi.org/10.1016/J.JALLCOM.2020.156938>.
- [2] Z. T. Karipbayev, K. Kumarbekov, I. Manika, A. Daultebekova, A. L. Kozlovskiy, D. Sugak, S. B. Ubizskii, A. Akilbekov, Y. Suchikova, and A. I. Popov. “Optical, structural, and mechanical properties of  $Gd_3Ga_5O_{12}$  single crystals irradiated with  $^{84}Kr^+$  ions.”. *Physica Status Solidi (B)*, 259(8):2100415, 2022. DOI: <https://doi.org/10.1002/pssb.202100415>.
- [3] F. Maglia, V. Buscaglia, S. Gennari, P. Ghigna, M. Dapiaggi, A. Speghini, and M. Bettinelli. “Incorporation of trivalent cations in synthetic garnets  $A_3B_5O_{12}$  ( $A = Y, Lu-La, B = Al, Fe, Ga$ ).” *J. Phys. Chem. B*, 110(13):6561–6568, 2006. DOI: <https://doi.org/10.1021/jp055713o>.
- [4] R. Krsmanovic, V. A. Morozov, O. I. Lebedev, S. Polizzi, A. Speghini, M. Bettinelli, G. Tendeloo, and Van. “Structural and luminescence investigation on gadolinium gallium garnet nanocrystalline powders prepared by solution combustion synthesis.”. *Nanotechnology*, 18(32):325604, 2007. DOI: <https://doi.org/10.1088/0957-4484/18/32/325604>.
- [5] C. A. Cortes-Escobedo, A. M. Bolarin-Miro, F. S. D. Jesus, R. Valenzuela, E. P. Juarez-Camacho, I. L. Samperio-Gomez, and S. Ammar. “ $Y_3Fe_5O_{12}$  prepared by mechano-synthesis from different iron sources.”. *Advances in Materials Physics and Chemistry*, 03(01): 41–46, 2013. DOI: <https://doi.org/10.4236/ampc.2013.31a006>.
- [6] R. Deghdak, M. Bouchemat, M. Lahoubi, S. Pu, T. Bouchemat, and H. Otmani. “Sensitive magnetic field sensor using 2D magnetic photonic crystal slab waveguide based on BIG/GGG structure.”. *J. Comput. Electron.*, 16(2):392–400, 2017. DOI: <https://doi.org/10.1007/s10825-017-0965-z>.
- [7] S. G. Parker and C. T. M. Chang. “Properties of garnet materials for contiguous disk magnetic bubble memory devices.”. *J. Electrochem. Soc.*, 129(2):423–427, 1982. DOI: <https://doi.org/10.1149/1.2123872>.

- [8] Y. Hosoe, R. Imura, R. Suzuki, and T. Ikeda. "Garnet films for 64 Mb bubble memory devices." *IEEE Trans Magn.*, 25(5):4254–4256, 1989.  
DOI: <https://doi.org/10.1109/20.42586>.
- [9] D. Neupane, N. Kramer, R. Bhattarai, C. Hanley, A. K. Pathak, X. Shen, S. Karna, and S. R. Mishra. "Rare-earth doped  $Gd_3-xRE_xFe_5O_{12}$  (RE = Y, Nd, Sm, and Dy) garnet: structural, magnetic, magnetocaloric, and DFT study." *Ceramics*, 6(4):1937–1976, 2023.  
DOI: <https://doi.org/10.3390/ceramics6040120>.
- [10] K. P. Belov, S. A. Nikitin, E. V. Talalaeva, L. A. Chernikova, T. V. Kudryavtseva, V. V. Tikhonov, and V. I. Ivanovskii. "Determination of exchange interaction of sublattices in gadolinium iron-garnet on the basis of the magnetocaloric effect." *Sov. Phys. JETP USSR*, 34: 588–92, 1972.
- [11] V. K. Pecharsky, V. K. Pecharsky, K. A. Gschneidner, K. A. Gschneidner, A. O. Pecharsky, and A. M. Tishin. "Thermodynamics of the magnetocaloric effect." *Phys. Rev. B. Condens. Matter. Mater. Phys.*, 64(14):1444061–14440613, 2001.  
DOI: <https://doi.org/10.1103/PhysRevB.64.144406>.
- [12] K. Klinar, J. Y. Law, V. Franco, X. Moya, and A. Kitanovski. "Perspectives and energy applications of magnetocaloric, pyromagnetic, electrocaloric, and pyroelectric materials." *Adv. Energy Mater.*, page 2401739, 2024.  
DOI: <https://doi.org/10.1002/aenm.202401739>.
- [13] Y. Zhang, Y. Na, W. Hao, T. Gottschall, and L. Li. "Enhanced cryogenic magnetocaloric effect from 4f-3d exchange interaction in B-site ordered  $Gd_2CuTiO_6$  Double Perovskite Oxide." *Adv. Funct. Mater.*, page 2409061, 2024.  
DOI: <https://doi.org/10.1002/adfm.202409061>.
- [14] J. Lin, X. Wang, F. Chen, H. F. Li, and L. Li. "Designing gadolinium-transition metals-based perovskite type high entropy oxides with good cryogenic magnetocaloric performances." *J. Mater. Sci. Technol.*, 207:317–323, 2025.  
DOI: <https://doi.org/10.1016/J.JMST.2024.05.004>.
- [15] Y. Zhang, W. Hao, J. Lin, H. F. Li, and L. Li. "Geometrically frustrated  $Gd_2Ti_2O_4$  oxide: A comprehensive exploration of structural, magnetic, and magnetocaloric properties for cryogenic magnetic cooling applications." *Acta Mater.*, 272:119946, 2024.  
DOI: <https://doi.org/10.1016/J.ACTAMAT.2024.119946>.
- [16] Y. Zhang, W. Hao, C. Hu, X. Wang, X. Zhang, and L. Li. "Rare-earth-free  $Mn_{30}Fe_{20}-CuAl_{50}$  magnetocaloric materials with stable cubic CsCl-type structure for room-temperature refrigeration." *Adv. Funct. Mater.*, 33(52):2310047, 2023.  
DOI: <https://doi.org/10.1002/adfm.202310047>.
- [17] Y. Zhang, W. Hao, J. Shen, Z. Mo, T. Gottschall, and L. Li. "Investigation of the structural and magnetic properties of the  $GdCoC$  compound featuring excellent cryogenic magnetocaloric performance." *Acta Mater.*, 276:120128, 2024.  
DOI: <https://doi.org/10.1016/J.ACTAMAT.2024.120128>.
- [18] R. D. McMichael, J. J. Ritter, and R. D. Shull. "Enhanced magnetocaloric effect in  $Gd_3Ga_5-xFexO_{12}$ ." *J. Appl. Phys.*, 73(10): 6946–6948, 1993.  
DOI: <https://doi.org/10.1063/1.352443>.
- [19] McMichael R. D., Shull R. D., Swartzendruber L. J., Bennett L. H., and Watson R. E. "Magnetocaloric effect in superparamagnets." *J. Magn. Magn. Mater.*, 111(1–2):29–33, 1992.  
DOI: [https://doi.org/10.1016/0304-8853\(92\)91049-Y](https://doi.org/10.1016/0304-8853(92)91049-Y).
- [20] X. Jin, J. Zhao, L. Gao, H. Ma, O. Haschuluu, H. Zhu, Q. Li, T. Su, H. Zhu, O. Tegus, and J. Zhao. "Influence of high-pressure heat treatment on magnetocaloric effects and magnetic phase transition in single crystal  $Gd_3Ga_5O_{12}$ ." *J. Rare Earths.*, 2024.  
DOI: <https://doi.org/10.1016/J.JRE.2024.01.003>.
- [21] V. Provenzano, J. Li, T. King, E. Canavan, P. Shirron, M. DiPirro, and R. D. Shull. "Enhanced magnetocaloric effects in  $R_3(Ga_{1-x}Fe_x)_5O_{12}$  ( $R=Gd, Dy, Ho; 0 < x < 1$ ) nanocomposites." *J. Magn. Magn. Mater.*, 266(1–2):185–193, 2003.  
DOI: [https://doi.org/10.1016/S0304-8853\(03\)00470-0](https://doi.org/10.1016/S0304-8853(03)00470-0).
- [22] M. H. Phan, M. B. Morales, C. N. Chinnasamy, B. Latha, V. G. Harris, and H. Srikanth. "Magnetocaloric effect in bulk and nanostructured  $Gd_3Fe_5O_{12}$  materials." *J. Phys. D. Appl. Phys.*, 42(11):115007, 2009.  
DOI: <https://doi.org/10.1088/0022-3727/42/11/115007>.
- [23] P. Schiffer, A. P. Ramirez, D. A. Huse, P. L. Gammel, U. Yaron, D. J. Bishop, and A. J. Valentino. "Frustration induced spin freezing in a site-ordered magnet: gadolinium gallium garnet." *Phys Rev. Lett.*, 74:2379–2382, 1995.  
DOI: <https://doi.org/10.1103/PhysRevLett.74.2379>.
- [24] A. P. Ramirez. "Strongly geometrically frustrated magnets." *Annu. Rev. Mater. Res.*, 24(24):453–480, 1994.  
DOI: <https://doi.org/10.1146/annurev.ms.24.080194.002321>.
- [25] T. Numazawa, K. Kamiya, T. Okano, and K. Matsumoto. "Magnetocaloric effect in  $(DyxGd_{1-x})_3Ga_5O_{12}$  for adiabatic demagnetization refrigeration." *Physica B Condens. Matter.*, 329–333(II): 1656–1657, 2003.  
DOI: [https://doi.org/10.1016/S0921-4526\(02\)02447-X](https://doi.org/10.1016/S0921-4526(02)02447-X).
- [26] V. Singh, G. Sivaramaiah, N. Singh, M. Mohapatra, D. A. Hakeem, M. S. Pathak, and J. L. Rao. "EPR and optical investigation of ultraviolet-emitting  $Gd_3Ga_5O_{12}$  garnet." *J Mater Sci: Mater Electron*, 29(2):944–951, 2018.  
DOI: <https://doi.org/10.1007/s10854-017-7992-1>.
- [27] K. Ghimire, H. F. Haneef, R. W. Collins, and N. J. Podraza. "Optical properties of single-crystal  $Gd_3Ga_5O_{12}$  from the infrared to ultraviolet." *Physica Status Solidi (B)*, 252(10):2191–2198, 2015.  
DOI: <https://doi.org/10.1002/pssb.201552115>.
- [28] M. Pang and J. Lin. "Growth and optical properties of nanocrystalline  $Gd_3Ga_5O_{12}:Ln$  ( $Ln=Eu^{3+}, Tb^{3+}, Er^{3+}$ ) powders and thin films via Pechini sol-gel process." *J. Cryst. Growth*, 284(1–2):262–269, 2005.  
DOI: <https://doi.org/10.1016/J.JCRYSGRO.2005.07.007>.
- [29] E. E. Hellstrom, R. D. Ray II, and C. Zhang. "Preparation of gadolinium gallium garnet [ $Gd_3Ga_5O_{12}$ ] by solid-state reaction of the oxides." *J. Am. Ceram. Soc.*, 72(8):1376–1381, 1989.  
DOI: <https://doi.org/10.1111/j.1151-2916.1989.tb07656.x>.
- [30] P. Jani aqnd H. Desai, B. S. Madhukar, and A. Tanna. "Investigations of calcium ferrite nanoparticles synthesized by sol-gel auto combustion and solution mixture methods." *Mater. Res. Innovations*, 26(3): 189–195, 2022.  
DOI: <https://doi.org/10.1080/14328917.2021.1932318>.
- [31] A. R. Tanna, K. M. Sosa, and H. H. Joshi. "Study of superparamagnetic nano particles of  $Mn_xCo_{1-x}Fe_2O_4$  ferrite system prepared by co-precipitation technique." *Mater. Res. Express*, 4(11):115010, 2017.  
DOI: <https://doi.org/10.1088/2053-1591/aa9393>.
- [32] A. E. Danks, S. R. Hall, and Z. Schnepf. "The evolution of 'sol-gel' chemistry as a technique for materials synthesis." *Mater. Horiz.*, 3(2):91–112, 2016.  
DOI: <https://doi.org/10.1039/C5MH00260E>.
- [33] A. C. Larson and R. B. Von Dreele. "General Structure Analysis System (GSAS)." *Los Alamos National Laboratory Report LAUR*, 2004.
- [34] Md. I. Ahmad and S. S. Bhattacharya. "Size effect on the lattice parameters of nanocrystalline anatase." *Appl. Phys. Lett.*, 95(19): 191906, 2009.  
DOI: <https://doi.org/10.1063/1.3261754>.
- [35] C. F. Holder and R. E. Schaak. "Tutorial on powder x-ray diffraction for characterizing nanoscale materials." *ACS Nano*, 13(7): 7359–7365, 2019.  
DOI: <https://doi.org/10.1021/acsnano.9b05157>.

- [36] S. Mustapha, M. M. Ndamitso, A. S. Abdulkareem, J. O. Tijani, D. T. Shuaib, A. K. Mohammed, and A. Sumaila. "Comparative study of crystallite size using Williamson-Hall and Debye-Scherrer plots for ZnO nanoparticles.". *Adv. Nat. Sci.: Nanosci. Nanotechnol.*, 10(4): 045013, 2019.  
DOI: <https://doi.org/10.1088/2043-6254/ab52f7>.
- [37] G. C. Bleier, J. Watt, C. K. Simocko, J. M. Lavin, and D. L. Huber. "Reversible magnetic agglomeration: A mechanism for thermodynamic control over nanoparticle size.". *Angew. Chem.*, 57(26): 7678–7681, 2018.  
DOI: <https://doi.org/10.1002/anie.201800959>.
- [38] E. W. Lim and R. Feng. "Agglomeration of magnetic nanoparticles.". *J. Chem. Phys.*, 28:136(12):124109, 2012.  
DOI: <https://doi.org/10.1063/1.3697865>.
- [39] W. Lu, H. Zhou, G. Chen, J. Li, Z. Zhu, Z. You, and C. Tu. "Photoluminescence properties of neat and Dy<sup>3+</sup>-Doped Gd<sub>3</sub>Ga<sub>5</sub>O<sub>12</sub> nanocrystals.". *J. Phy. Chem. C.*, 113(9):3844–3849, 2009.  
DOI: <https://doi.org/10.1021/jp8082369>.
- [40] C. Cascales, M. T. Fernandez Diaz, and M. A. Monge. "Low-Temperature magnetic ordering in rare-earth copper germanates R<sub>2</sub>CuGe<sub>4</sub>O<sub>12</sub>, R = Ho". *Er. Chem. Mater.*, 12(11):3369–3375, 2000.  
DOI: <https://doi.org/10.1021/cm0011209>.
- [41] J. Jensen and A. R. Mackintosh. "Rare earth magnetism structures and excitations.". *Clarendon press • Oxford.*, 1991.  
DOI: <https://doi.org/10.1093/oso/9780198520276.001.0001>.
- [42] P. M. Savaliya, S. R. Ajudiya, J. Sahoo, S. Katba, and A. R. Tanna. "Structural and magnetic properties of GdFeO<sub>3</sub> nanomaterial prepared through one-step sol-gel auto combustion technique.". *J. Sol-gel Sci. Technol.*, 110(2):434–442, 2024.  
DOI: <https://doi.org/10.1007/s10971-024-06367-z>.
- [43] O. A. Petrenko, C. Ritter, M. Yethiraj, and D. McK Paul. "Investigation of the low-temperature spin-liquid behavior of the frustrated magnet gadolinium gallium garnet.". *Phys. Rev. Lett.*, 80(20): 4570–4573, 1998.  
DOI: <https://doi.org/10.1103/PhysRevLett.80.4570>.
- [44] S. Hov, H. Bratsberg, and A. T. Skjeltorp. "Magnetic phase diagram of gadolinium gallium garnet.". *J. Magn. Magn. Mater.*, 15–18(PART 1):455–456, 1980.  
DOI: [https://doi.org/10.1016/0304-8853\(80\)91128-2](https://doi.org/10.1016/0304-8853(80)91128-2).
- [45] S. R. Dunsiger, J. S. Gardner, J. A. Chakhalian, A. L. Cornelius, M. Jaime, R. F. Kiefl, R. Movshovich, W. A. Macfarlane, R. I. Miller, J. E. Sonier, and B. D. Gaulin. "Low temperature spin dynamics of the geometrically frustrated antiferromagnetic garnet Gd<sub>3</sub>Ga<sub>5</sub>O<sub>12</sub>". *Phys. Rev. Lett.*, 85(16):3504–3507, 2000.  
DOI: <https://doi.org/10.1103/PhysRevLett.85.3504>.
- [46] N. K. Chogondahalli Muniraju, R. Baral, Y. Tian, R. Li, N. Poudel, K. Gofryk, N. Barisic, B. Kiefer, J. H. Jr. Ross, and H. S. Nair. "Magnetocaloric effect in a frustrated Gd-garnet with no long-range magnetic order.". *Inorg. Chem.*, 59(20):15144–15153, 2020.  
DOI: <https://doi.org/10.1021/acs.inorgchem.0c02074>.
- [47] C. P. Reshmi, S. Savitha Pillai, K. G. Suresh, and M. R. Varma. "Magnetic and magnetocaloric properties of Gd<sub>3-x</sub>TbxGa<sub>5</sub>O<sub>12</sub> (x=0, 1, 2, 3) garnets.". *J. Magn. Magn. Mater.*, 324(12):1962–1966, 2012.  
DOI: <https://doi.org/10.1016/J.JMMM.2012.01.030>.
- [48] M. D. Kuz'min and A. M. Tishin. "Magnetic refrigerants for the 4.2-20 K region: Garnets or perovskites?". *J. Phys. D. Appl. Phys.*, 24(11):2039–2044, 1991.  
DOI: <https://doi.org/10.1088/0022-3727/24/11/020>.
- [49] W. Dunhui, T. Shaolong, H. Songling, Z. Jianrong, and D. Youwei. "The magnetic phase transition and the low-field Arrott plots of (Gd<sub>x</sub>Dy<sub>1-x</sub>)Co<sub>2</sub> compounds.". *J. Magn. Magn. Mater.*, 268(1–2): 70–74, 2004.  
DOI: [https://doi.org/10.1016/S0304-8853\(03\)00474-8](https://doi.org/10.1016/S0304-8853(03)00474-8).
- [50] V. Franco, J. S. Blazquez, and A. Conde. "Field dependence of the magnetocaloric effect in materials with a second order phase transition: A master curve for the magnetic entropy change.". *Appl. Phys. Lett.*, 89(22):222512, 2006.  
DOI: <https://doi.org/10.1063/1.2399361>.